geoconvention
Calgary • Canada • May 15-19 2017

HTI anisotropy in heterogeneous elastic model and homogeneous equivalent model

Sitamai, W. Ajiduah, Gary, F. Margrave and Pat, F. Daley*
CREWES/University of Calgary.

Summary

In this study, we compared a 3D finite-difference elastic modeling of an isotropic heterogeneous elastic model with a 3D finite difference anisotropic modeling of an homogeneous equivalent model in order to verify the suitability of these two modeling approaches for anisotropic studies. We focused on P-wave and PS-wave reflections from the top and bottom of the fractured HTI medium. Although, geophysicists often prefer to use anisotropic homogeneous equivalent models for various seismic modeling and imaging tasks, there are however some benefits of using heterogeneous models over anisotropic homogeneous equivalent models. We show that the anisotropic equivalent modeling predicts strong interbed multiples and multimodes which are much weaker in the heterogeneous elastic model. This is because a heterogeneous medium will cause irregular scattering of multiples and multimode events, thus diminishing these events. We inferred that in some circumstances modeling using heterogeneous elastic models might be of higher processing and imaging value than with equivalent media.

Introduction

Fracture detection and the estimation of fracture properties are important for reservoir characterization, hydrocarbon production and CO_2 storage. Studies have shown that azimuthal variation in seismic attributes (such as velocity, amplitude, and frequency) of P and S-wave data can be used as an indicator of azimuthal anisotropy (Daley and Hron, 1977; Ruger 1996; Bakulin et. al. 2000; Qian et al., 2007; Mahmoudian, et. al. 2013; Al Dulaijan et. al. 2016). Parallel vertical crack orientations can occur when the vertical stress becomes greater than the minimum horizontal stress. A medium containing vertically aligned fractures with scale length much less than the scale of the seismic wavelength can be modelled by an homogeneous equivalent azimuthally anisotropic medium. The use of azimuthal seismic anisotropy to detect natural fractured reservoirs using equivalent medium theory has been studied by many authors (e.g. Hudson, 1981; Schoenberg and Douma, 1988; Liu et. al 2000).

We used SINTEF TIGER staggered-grid finite-difference numerical modeling scheme to generate synthetic three-component 3D datasets and compared datasets from both the isotropic heterogeneous elastic model and anisotropic homogeneous equivalent media and compared the results from these two models. The HTI parameters of the anisotropic equivalent medium were obtained from a linear slip model proposed by Schoenberg and Muir (1989) and tested and verified by Carcione et. al. (2012) for any general anisotropic medium by numerical simulation. We studied the PP and PS- moveout and AVO behavior of these two modeling with the aim of using the modelling results as guidance for future modeling, processing and interpretation of anisotropic response of orthorhombic models with finely layered overburden.

Method

Figure 1 shows the three-layer model used in this synthetic study. A periodic isotopic heterogeneous elastic fractured model (hereafter simply referred to as an elastic medium) and an anisotropic homogenous equivalent medium obtained from Schoenberg and Muir linear slip method (hereafter simply referred to as an equivalent medium) were created. The top layer and bottom layer are isotropic, while the second layer is a 400m thick HTI layer modeling vertical fracturing. Fracture spacing is at a

20m interval and fracture strike is 0 degrees in the azimuthal plane. The offset range is from 20m to 2000m. The source, an explosive P-source with a 15 Hz Ricker spectrum, is located at the center of the model, at depth 40m. This gives full azimuthal coverage through all 360 degrees. 3C receivers were placed on each of the grid points and buried at source depth. 3D shot records were generated for both the elastic and the equivalent model. The parameters of equivalent model and elastic model are shown in Table 1 below. Modeling was done with a grid size of 201x201x101. The recorded 3D Z, X, Y datasets were later bandpass filtered and rotated into ZRT components. We then applied a 2D linear interpolation at every time-slice and translate the dataset from its acquisition domain to the offset-azimuth domain in order to obtained azimuthal scans and radial scans of datasets ($Z_{(t,r,\varphi)}$, $R_{(t,r,\varphi)}$ and $T_{(t,r,\varphi)}$) for further amplitude/time picking analysis and interpretations.

Table 1: Parameters of Model used in modeling.

	Heterogeneous elastic model	Homogeneous equivalent model
Layer1	$Vp = 3500m/s, Vs = 2140m/s,\ \rho = 2200kg/m^3$	same
HTI Layer	$Vp_1 = 4700m/s, Vs_1 = 3980m/s, \rho_1 = 2500kg/m$ $Vp_2 = 4210m/s,\ Vs_2 = 2430m/s, \rho_2 = 2300kg/m$	$Vp_0 = 4438m/s, Vs_0 = 2762m/s, \rho^c = 2401kg/$ $\epsilon^c = .0034, \gamma^c = .0607, \delta^c = -.0545$
Layer3	$Vp = 5000m/s, Vs = 3300m/s, \rho = 2900kg/m^3$	same

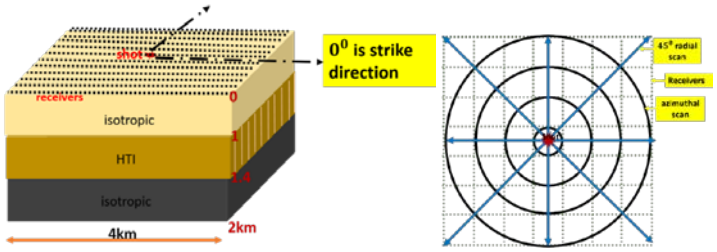

Figure 1. Three-layer model and survey geometry (left) of shot and receivers showing fracture strike directions. The diagram on the right shows the plan view of what the azimuthal and radial scans look like.

Examples

Figure 2 (a-c) shows the common-azimuth radial scans of the 3C shot gathers along azimuths 0, 15, 60, 90, 105, and 150 degrees to the fracture strike with the fracture strike and normal at 0 and 90 degrees respectively. Vertical (Z), radial (R), and transverse (T) components are shown. Modeling predicts exact arrival times as raytracing from the top and base of the fractured media for PP (solid red lines), PPpp (dashed red lines), PS (solid blue lines), and PPss reflections (dashed blue lines) for both models. The solid green lines are the multimodes. Both modeling gave correct moveout and AVO behavior however the equivalent modeling appears noisier than the elastic modeling. Notice that the transverse component is zero along 0° and 90° indicating the principal planes of fracturing. Also notice that the transverse datasets measured along non-principal planes are not zero, revealing shear-wave birefringence. It is interesting to add that modeling with an isotropic heterogeneous elastic modeling unlike the homogenous equivalent modeling, produced a better result without the amplification of multiples and multimodes.

Figure 3 (a-c) shows the common offset azimuthal scans of the vertical, radial and transverse datasets at offset of 1.6km for elastic modeling (left) and equivalent modeling (right). The red line and the blue lines indicate the PP and PS primary arrivals from the top and base of the HTI layer and the location of picks.

The signature of shear-wave splitting is seen as azimuthal time variation on the $ZRT_{(t,r,\varphi)}$ datasets, but is most clearly diagnosed from the polarity changes observed along the principal axes on the transverse component. We see an overlap between the fast (PS1) and slow (PS2) shear waves in the $Z_{(t,r,\varphi)}$ and $R_{(t,r,\varphi)}$ azimuthal scans indicating shear-wave birefringence from the top and bottom of the HTI layer and seen as sinusoidal events at time 1 seconds and time 1.2 seconds. The transverse component (figure 3c) has a distinctly different character. At any intermediate azimuths, the transverse dataset shows shear-wave splitting and the fast and slow shear waves are opposite in polarity. There is no shear wave splitting along isotropy (green arrow) and symmetry axis (orange arrow) where amplitudes drop to zero. These directions are the principal directions or the natural coordinates of fracturing. This characteristic polarity reversal was exploited in several different analyses in this study to determine fracture orientation from shear wave splitting and a key element for recognizing an HTI system. Also, notice the strong multimode event appearing at 1.3 seconds in the elastic modeling (left) which appear much stronger in the equivalent medium (right). This is caused by the attenuation due to lateral heterogeneity and irregular scattering within the heterogeneous elastic fractured model. In addition, the transverse component of the equivalent model seems noisier than the elastic model showing the effect of amplified multiples arising from using a homogeneous equivalent model.

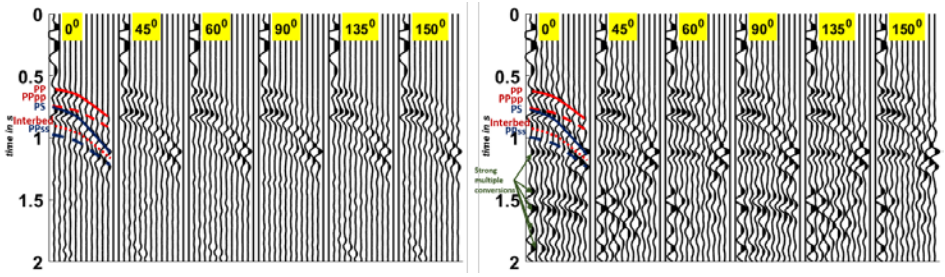

Figure 2a: Vertical, Z, component radial scans showing offset variation at various fixed azimuths. The elastic model is at left and the equivalent model at right. The yellow labels are the azimuthal values in degree. Red and Blue lines are the P and PS reflections. The green lines are the multiples and multimode; stronger in the homogeneous model (right) than in the heterogeneous model (left). The moveout arrivals of the primary reflections are the same in both models for all datasets.

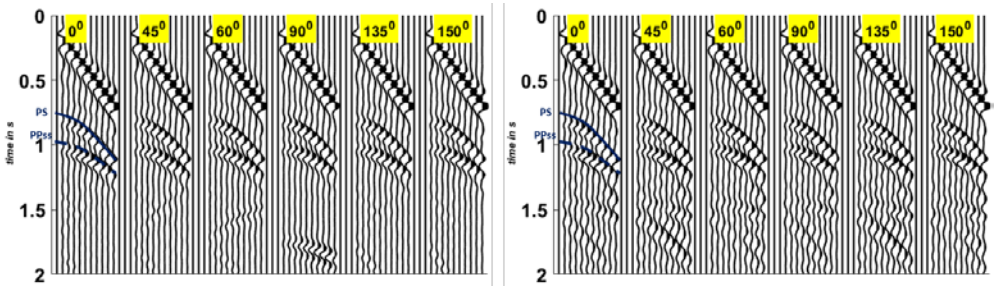

(2b) Similar to 4a but the R (radial) components.

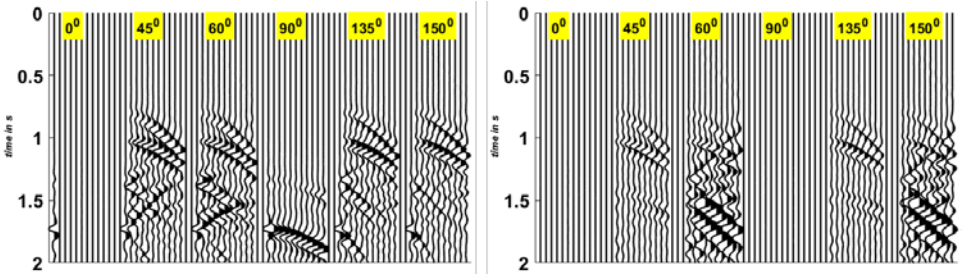

(2c) Similar to 4a but the transverse T components

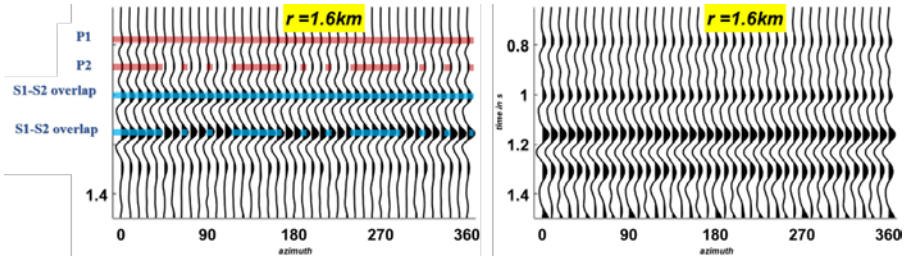

Fig 3a. Z-azimuthal scans. The red and blue line indicates PP and PS primary arrivals from HTI interfaces. The sinusoidal appearance of P waves shows fracture-induced PP azimuthal anisotropy whose imprint grows at increasing offset to depth ratio. Notice the strong multimode event appearing at 1.3 seconds in both models.

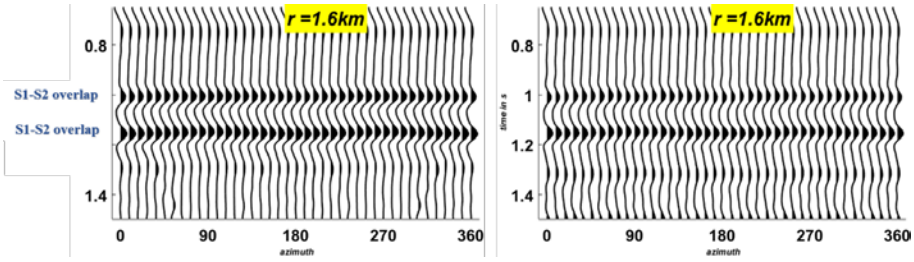

Fig 3b. R-azimuthal scan of elastic modeling (left) and equivalent modeling (right), showing overlap of PS1 and PS2 mode. The sinusoidal appearance at time 1 seconds is the side effect of the overlap between S1 and S2 modes with a time delay between them. Same as at time 1.2 seconds.

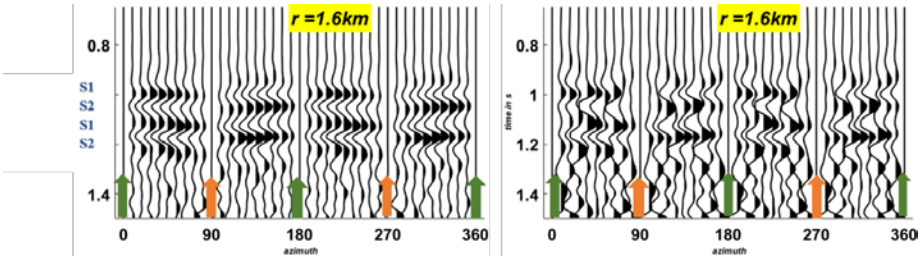

Fig 3c. T-azimuthal scan, showing clear separation of S1 and S2 modes indicating shear wave birefringence. The polarity of both the fast and slow shear waves reverses across the symmetry planes. The green and orange arrows represent the isotropy and symmetry respectively.

Conclusions

We have successfully carried out a 3D numerical modeling comparison of a vertically fractured isotropic heterogeneous elastic model and a homogeneous equivalent model computed from Schoenberg and Muir's linear slip theory with the goal of understanding the benefits of using either of these model types in understanding anisotropic responses and noise in multicomponent data. We observed that both model give similar moveout and AVO behaviour, however the homogeneous equivalent modeling is susceptible to strong multiple and multimode interferences which are attenuated in heterogeneous models due to irregular scattering effect caused by the fractured medium heterogeneity. We infer that in some circumstances modeling using heterogeneous elastic models might be of higher imaging value than with equivalent media.

Acknowledgements

This work was funded by CREWES industrial sponsors and NSERC (Natural Science and Engineering Research Council of Canada) through the grant CRDPJ 461179-13. The authors also thank SINTEF for providing the TIGER finite-difference modeling software. The first author gratefully acknowledge Kevin Hall, Kevin Bertram, Faranak Mahmoudian and Raul Cova for their assistance.

References

Al Dulaijan and Margrave, G. F. 2016, VVAZ analysis for seismic anisotropy in the Altamont-Bluebell Field, 86th Annual International Meeting, SEG, Expanded Abstracts.

Backus, G. E., 1962, Long-wave elastic anisotropy produced by horizontal layering: Journal of Geophysical Research, 67, 4427–4440.

Bakulin, A., Grechka, V., and Tsvankin, I., 2000, Estimation of fracture parameters from reflection seismic data. Part I: HTI model due to a single fracture set: Geophysics, 65, 1788–1802.

Carcione, J.M., Picotti, S., Cavallini, F., Santos, J.E., 2012. Numerical test of the Schoenberg-Muir theory. Geophysics 77, 27-35.

Daley, P.F. and Hron, F., 1977, Reflection and transmission coefficients for transversely isotropic media, Bulletin of the Seismological Society of America, **67**, 661-675.

Hudson, J. A., 1981, Wave speeds and attenuation of elastic waves in material containing cracks. Geophysical Journal Royal Astronaut Society, 64, 133 – 150.

Liu, E., Hudson, J. A., and Pointer, T., 2000. Equivalent medium representation of fractured rock: Journal of Geophysical Research, 105, 2981 – 3000.

Mahmoudian, F., Margrave, G.F., Wong, J., and Henley, D.C, 2013, Fracture orientation and intensity from AVAz inversion: A physical modeling study. 83th Annual International Meeting, SEG, Expanded Abstracts.

Qian, Z., Li, X-Y., Chapman, M., 2007, Azimuthal variations of PP- and PS-wave attributes: a synthetic study: 77th Annual International Meeting, SEG, Expanded Abstracts, 184–187.

Rüger A. 1996, Variation of P-wave reflectivity with offset and azimuth in anisotropic media: 66th Annual International Meeting, SEG, Expanded Abstracts, 15, 1810–1813.

Schoenberg, M. and Douma, J., 1988, Elastic-wave propagation in media with parallel fractures and aligned cracks: Geophysical Prospecting, EAGE., 36,571-590.

Schoenberg, M., and Muir, F., 1989, A calculus for finely layered media: Geophysics, 54, 581–589,